



Ferroptosis is partially responsible for dexamethasone-induced T cell ablation, but not osteoporosis in larval zebrafish

Wenyu Miao^{a,c,*}, Lingling He^c, Yong Zhang^c, Xiaoyu Zhu^c, Yangming Jiang^{b,d}, Pengpeng Liu^{b,d}, Tao Zhang^c, Chunqi Li^c

^a School of Public Health, Zhejiang University School of Medicine, Hangzhou, Zhejiang 310058, China

^b Zhejiang Provincial Key Laboratory of Biosafety Detection for Market Regulation, Hangzhou, Zhejiang 310018, China

^c Hunter Biotechnology, Inc., Hangzhou, Zhejiang 310051, China

^d Zhejiang Fangyuan Test Group Co., Ltd, Hangzhou, Zhejiang 310018, China

ARTICLE INFO

Edited by: Yong Liang

Keywords:

Zebrafish larvae
Ferroptosis
Immunotoxicity
Osteoporosis
Caudal regeneration

ABSTRACT

Glucocorticoids (GCs) have been widely detected in the aquatic system. However, the hazardous effects of GCs on aquatic organisms were underestimated, and the mechanisms of GCs-induced toxic effects in fish were largely unknown. The zebrafish larvae at 3 dpf were exposed to dexamethasone (DEX) for 48 h, and the toxic effects and the underlying mechanisms were investigated in the current study. The T cells were ablated in zebrafish larvae after being treated with 1, 3, 10, 30 and 100 μM of DEX for 48 h. In addition, osteoporosis was induced and the regeneration of the caudal fin was inhibited, by 48 h-exposure to 10, 30 and 100 μM of DEX. The transcriptomic analysis, biochemical parameters and gene expression profiles revealed that ferroptosis possibly contributed to the DEX-induced toxic effects in zebrafish larvae. Finally, Fer-1 treatment partially attenuated the DEX-induced T cell ablation, but not osteoporosis in zebrafish larvae. Taken together, the current study proved the toxic effects of DEX on zebrafish larvae, and elucidated that ferroptosis was involved in DEX-induced toxicity, providing strong evidence for the toxic effects of GCs on aquatic organisms.

1. Introduction

Endocrine-disrupting chemicals (EDCs) have attracted concern in recent decades, since they were demonstrated to interfere with the normal function of the endocrine system in organisms at low concentrations, and resulted in multiple toxic effects, such as reproductive toxicity, developmental toxicity, mutagenicity, immunotoxicity, carcinogenicity, and neurotoxicity (Choi et al., 2004; Lisco et al., 2021). Compared with sex hormones, various glucocorticoids (GCs) are more widely used in humans and animals. Because the GCs are partially metabolized, the undecomposed compounds may be excreted via urine or feces (Bamberg et al., 2001). In addition, non-metabolized GCs in external products can be washed off from the skin (Weizel et al., 2018). As a consequence, natural and synthetic GCs have been widely detected in the aquatic system (Shen et al., 2020). Generally, the levels of individual GCs detected in surface water ranged from 0.1 to 50 ng/L (Jia et al., 2016; Weizel et al., 2018). While some highly prescribed compounds are ubiquitous in the aquatic system with extremely high concentrations. For instance, betamethasone was reported to be higher than

700 ng/L in a river in Brazil (Foureaux et al., 2019) and up to 1720 ng/L in hospital wastewaters (Macikova et al., 2014). As a family consisting of a huge number of members, the concentration of GCs in the aquatic system is largely underestimated.

GCs exert functions mainly through the activation of the glucocorticoid receptor (GR), and also crosstalk with other hormone receptors, such as the mineralocorticoid receptor (MR) (Schaaf et al., 2009; Pippala et al., 2011). Previous studies demonstrated that the teleost fish express both the GR and MR (Bury et al., 2003; Greenwood et al., 2003; Sturm et al., 2005). For instance, two GRs (GR α and GR β) and one MR have been sequenced in zebrafish (Chatzopoulou et al., 2017; Katsu et al., 2018). Activation of the GR and MR in fish by endogenous corticosteroid hormones mediates various physiological functions, including stress response, energy metabolism, immune response and osmoregulation (Mommensen et al., 1999; Takahashi et al., 2013). The adverse effects of exogenous GCs in humans have been widely reported, such as musculoskeletal side effects (Van Staa et al., 2000; Weinstein, 2012; Schakman et al., 2008), endocrine and metabolic side effects (Olefsky et al., 1976; Arnaldi et al., 2010; Da Silva et al., 2006), gastrointestinal side effects

* Correspondence to: Hunter Biotechnology, Inc., Jiangling Road #88, Hangzhou, Zhejiang 310051, China.

E-mail address: miaowuy1988@163.com (W. Miao).

<https://doi.org/10.1016/j.ecoenv.2022.113872>

Received 27 April 2022; Received in revised form 15 June 2022; Accepted 7 July 2022

0147-6513/© 2022 The Author(s). Published by Elsevier Inc. This is an open access article under the CC BY-NC-ND license (<http://creativecommons.org/licenses/by-nc-nd/4.0/>).

(Piper et al., 1991; Sadr-Azodi et al., 2013), cardiovascular side effects (Huscher et al., 2009; Wei et al., 2004) and immunologic side effects (Stuck et al., 1989; Grossi et al., 2013). However, as a new class of endocrine disruptors, GCs in the aquatic system have received little attention until recent years (Zhang et al., 2019). In 2011, Kugathas et al. (2011) firstly reported that the glucose level was increased and the number of leucocytes was decreased significantly in the fathead minnows exposed to 1 µg/L prednisolone or beclomethasone for 21 days. Whereafter, more and more toxic effects induced by exogenous GCs-exposure in fish were reported, such as preterm hatching, deformations, increase in heart rate, immune suppression and osteoporosis (de Vrieze et al., 2014; Zhao et al., 2016; Zhang et al., 2017; Willi et al., 2018). Similar to what has been observed in humans, immune suppression and osteoporosis were the most frequently reported toxic effects induced by GCs in aquatic organisms (Liu et al., 2013; Qi et al., 2019; Rosa et al., 2021). However, the potential mechanisms of the toxic effects induced by GCs in aquatic organisms are largely unknown.

Zebrafish are widely used in evaluating the aquatic toxicity of hazardous materials (Hill et al., 2005; Bambino et al., 2017). In the present study, the toxic effects of a commonly used synthetic glucocorticoid, dexamethasone (DEX) were evaluated in larval zebrafish. The alteration in gene expression was elucidated using RNA-seq, and the signal pathways and biological processes modulated by DEX were analyzed using Kyoto Encyclopedia of Genes and Genomes (KEGG) pathway enrichment and Gene Ontology (GO) analysis. Finally, the mechanisms were further confirmed by ELISA, q-PCR and phenotype identification. Our findings elucidated the new mechanisms involved in DEX-induced toxic effects and further strengthened the evidence of DEX-induced aquatic toxicity, which might appeal to prevent the discharge of waste into the environment.

2. Materials and methods

2.1. Chemicals

Dexamethasone, Fer-1, NAC and GSH were purchased from Aladdin (Shanghai, China). Calcein was purchased from Dojin (Tokyo, Japan). Alizarin red S was purchased from Sigma Aldrich (Saint Louis, MO, USA). CM-H2DCFDA was purchased from ThermoFisher Scientific (Waltham, MA, USA).

2.2. Zebrafish and embryos

The zebrafish strains used in this study were wild-type AB, Tg (OlaSp7:nlsGFP), Tg (rag2:DsRed) and Tg (Col2a1a:eGFP). Tg (OlaSp7:nlsGFP) is a transgenic zebrafish line that expresses enhanced green fluorescent protein (eGFP) in bone (Spoorendonk et al., 2008). Tg (rag2:DsRed) is a transgenic zebrafish line that expresses red fluorescent protein under the control of the rag2 promoter (Zhang et al., 2015). Tg (Col2a1a:eGFP) is a transgenic zebrafish line that expresses eGFP in cartilage (Askary et al., 2015). All the zebrafish were provided by the China Zebrafish Resource Center (Wuhan, China). The zebrafish were maintained at 28 ± 1 °C with a light/dark photoperiod of 14 h/10 h. Healthy embryos produced by the pair-wise mated adults were collected and kept in E3 medium until the further test. This work has been approved by the ethics committee of Hunter Biotechnology, Inc. (AAALAC001458) and a proof/certificate of approval is available upon request.

2.3. Analysis of DEX-induced T cell ablation in Tg (rag2:DsRed) larvae

Larvae at 3 dpf were exposed to 1, 3, 10, 30 and 100 µM of DEX at a density of 30 larvae/well in 3 ml E3 medium for 48 h. The control group was treated with an equal volume of DMSO (0.1% v/v). Fifteen larvae per well were randomly selected and embedded in 3% methylcellulose. The fluorescent images were captured by Nikon AZ100 fluorescent

microscopy (Nikon, Japan). The fluorescence in the thymus was quantified using NIS-ElementsD 3.20 software (Nikon, Japan).

2.4. Analysis of DEX-induced osteoporosis in AB, Tg (OlaSp7:nlsGFP) and Tg (Col2a1a:eGFP) larvae

Larvae at 3 dpf were exposed to 1, 3, 10, 30 and 100 µM of DEX at a density of 30 larvae/well in 3 ml E3 medium for 48 h. The control group was treated with an equal volume of DMSO (0.1% v/v).

For the transgenic zebrafish, fifteen 5 dpf larvae per well were randomly selected and embedded in 3% methylcellulose. The fluorescent images were captured by Nikon AZ100 fluorescent microscopy (Nikon, Japan). The fluorescence of the osteoblasts in the head region of Tg (OlaSp7:nlsGFP) larvae and the fluorescence of the craniofacial cartilage of Tg (Col2a1a:eGFP) larvae were quantified using NIS-ElementsD 3.20 software (Nikon, Japan).

For calcein staining, the DEX-treated larvae of AB strain at 5 dpf were bathed in 3 ml of newly prepared staining solution (0.5 mg/ml in E3 medium, pH 7.0) for 5 min (Du et al., 2001). After being washed by E3 medium three times, fifteen larvae per well were randomly selected and embedded in 3% methylcellulose. The fluorescent images were captured by Nikon AZ100 fluorescent microscopy (Nikon, Japan) and the number of vertebrae was quantified.

For alizarin red staining, the DEX-treated larvae of AB strain at 5 dpf were euthanized with an overdose of MS 222, followed by fixed with 4% PFA in PBS for 2 h. The larvae were rinsed in 50% ethanol for 10 min and stained with 0.005% Alizarin red S in 1% KOH overnight. After being washed with PBS, the larvae were bleached with 1.5% H₂O₂/1% KOH for 20 min. Finally, the larvae were stained by using 50% glycerol/1% KOH for 2 h (Spoorendonk et al., 2008). Fifteen larvae per well were randomly selected and embedded in 3% methylcellulose. The fluorescent images were captured by Nikon AZ100 fluorescent microscopy (Nikon, Japan) and the number of vertebrae was quantified.

2.5. Analysis of caudal fin regeneration in AB larvae

Larvae at 3 dpf were anesthetized with 0.02% tricaine, and the caudal fins were cut off just posterior to the notochord, according to a previously reported method (Sun et al., 2018). The larvae were then immersed in 1, 3, 10, 30 and 100 µM of DEX at a density of 30 larvae/well in 3 ml E3 medium for 48 h. At the endpoint of DEX exposure, fifteen larvae per well were randomly selected and embedded in 3% methylcellulose. The optical images were captured by a Nikon AZ100 fluorescent microscopy (Nikon, Japan) and the area of regenerated caudal fin was quantified using Image J.

2.6. Morphological observation in AB larvae

Larvae at 3 dpf were exposed to 1, 3, 10, 30 and 100 µM of DEX at a density of 30 larvae/well in 3 ml E3 medium for 48 h. The control group was treated with an equal volume of DMSO (0.1% v/v). The optical images were captured by a Nikon AZ100 fluorescent microscopy (Nikon, Japan) and the body length was quantified using NIS-ElementsD 3.20 software (Nikon, Japan).

2.7. ROS measurement

Larvae at 3 dpf were exposed to 10, 30 and 100 µM of DEX at a density of 30 larvae/well in 3 ml E3 medium for 24 h, and then, ten larvae at 4 dpf were individually transferred to a 96-well plate containing 100 µl of DEX solution with 0.5 µg/ml CM-H2DCFDA and incubated for another 24 h. The fluorescence intensity of each well was measured at ex485 nm/em535 nm by using a microplate reader (Spark, TECAN, Männedorf, Switzerland) (Formella et al., 2018).

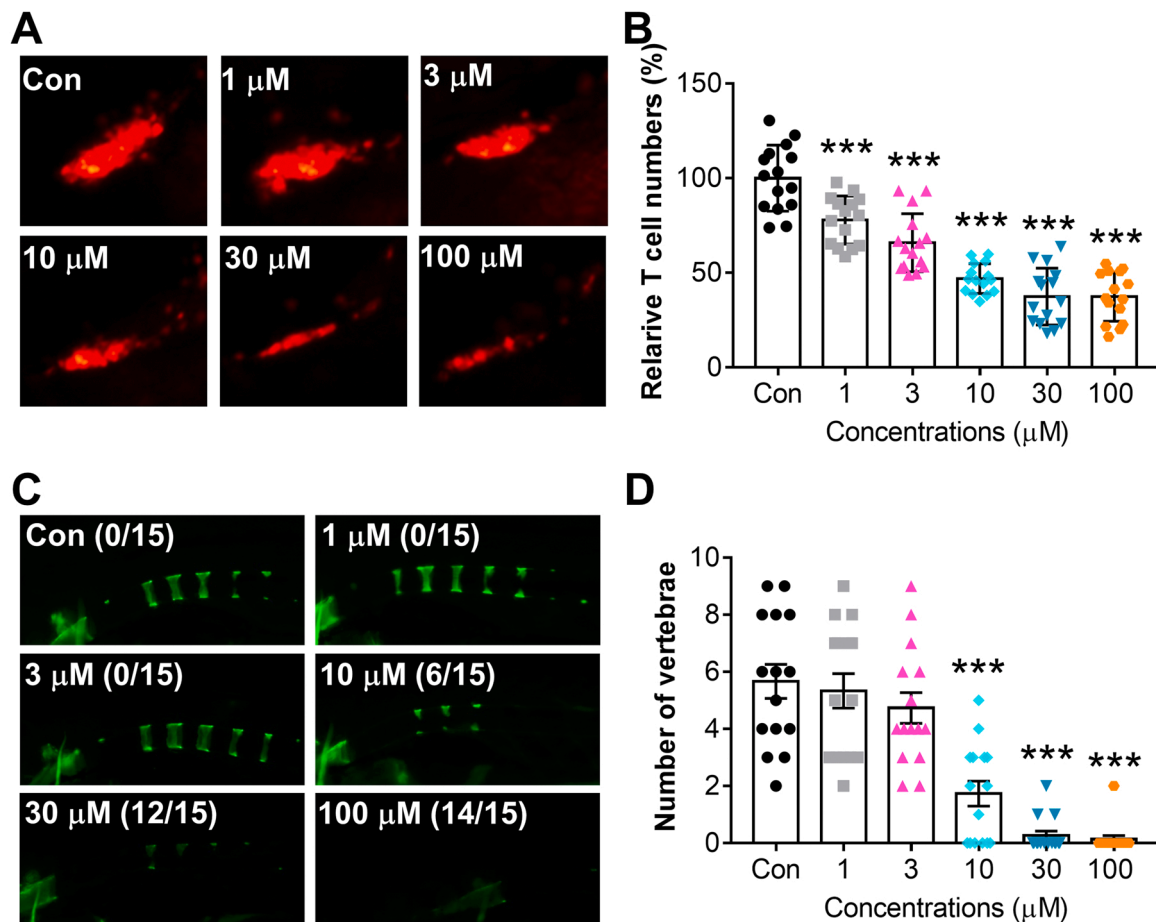


Fig. 1. The toxic effects of DEX on zebrafish larvae. (A) Representative images of the thymus of 5 dpf larvae treated with DEX for 48 h. (B) Quantitative data of (A), $n = 15$. (C) Representative images of the vertebrae stained by calcein in 5 dpf larvae treated with DEX for 48 h. (D) Quantitative data of (C), $n = 15$. Data were shown as means \pm SE. ** $p < 0.01$, *** $p < 0.001$, compared with the control group.

2.8. GSH measurement in AB larvae

Larvae at 3 dpf were exposed to 10, 30 and 100 μM of DEX at a density of 30 larvae/well in 3 ml E3 medium for 48 h. After euthanized with an overdose of MS 222, thirty larvae were homogenized in 100 μl of PBS using a homogenizer (65 Hz, 1 min). The homogenate was centrifuged at 5000 rpm for 10 min at 4 $^{\circ}\text{C}$, and the supernatant was collected for further test. The GSH content in the supernatant was detected using a commercial kit purchased from Nanjing Jiancheng Biotech (Nanjing, China), according to the manufacturer's instruction.

2.9. MDA measurement

Larvae at 3 dpf were exposed to 10, 30 and 100 μM of DEX at a density of 30 larvae/well in 3 ml E3 medium for 48 h. After euthanized with an overdose of MS 222, thirty larvae were homogenized in 60 μl of PBS using a homogenizer (65 Hz, 1 min). The homogenate was centrifuged at 5000 rpm for 10 min at 4 $^{\circ}\text{C}$, and the supernatant was collected for further test. The MDA content in the supernatant was measured using a commercial kit purchased from Nanjing Jiancheng Biotech (Nanjing, China), according to the manufacturer's instruction.

2.10. Transcriptomic analysis in AB larvae

Larvae at 3 dpf were exposed to 10 μM of DEX at a density of 30 larvae/well in 3 ml E3 medium for 48 h. Total RNA was extracted from thirty larvae using Trizol (Takara Biochemicals, Dalian, China) and the quantity and quality were assessed using NanoDrop 2000 (Thermo

Scientific, Fisher, MA, USA). The mRNA was enriched and fragmented, followed by reverse transcribed into cDNA. The cDNA was modified with adapters and amplified by PCR. The double-stranded PCR products from the previous step were heat-denatured and circularized by the splint oligo sequence to get the final library. The cDNA library was further sequenced using BGISEQ-500 platform in BGI tech (BGI-Shenzhen, China). After filtering with SOAPnuke (v1.5.2) (<https://github.com/BGI-flexlab/SOAPnuke>), the clean reads were obtained and stored in FASTQ format. The valid reads were mapped to the reference genome using HISAT2 (v2.0.4) (<http://www.ccb.jhu.edu/software/hisat/index.shtml>) and the expression level of the gene was calculated by RSEM (v1.2.12) (<https://github.com/deweylab/RSEM>). Finally, a more in-depth analysis of sequencing data was conducted, including GO (Gene Ontology) (<https://www.geneontology.org/>) and KEGG (<https://www.kegg.jp/>) enrichment analysis of annotated different expression genes. The significant levels of terms and pathways were corrected by Q value with a rigorous threshold (Q value ≤ 0.05).

2.11. Real-time quantitative PCR

Larvae at 3 dpf were exposed to 10 and 100 μM of DEX at a density of 30 larvae/well in 3 ml E3 medium for 48 h. After being extracted from thirty larvae using Trizol (Takara Biochemicals, Dalian, China), total RNA was quantified using NanoDrop 2000 (Thermo Scientific). cDNA was synthesized from two μg of RNA using FastKing RT kit (Tiangen Biotech, China), according to the manufacturer's instruction. The expression levels of target genes were quantified using iTaq Universal SYBR Green (Bio-Rad, California, USA) on the Bio-Rad CFX Connect PCR

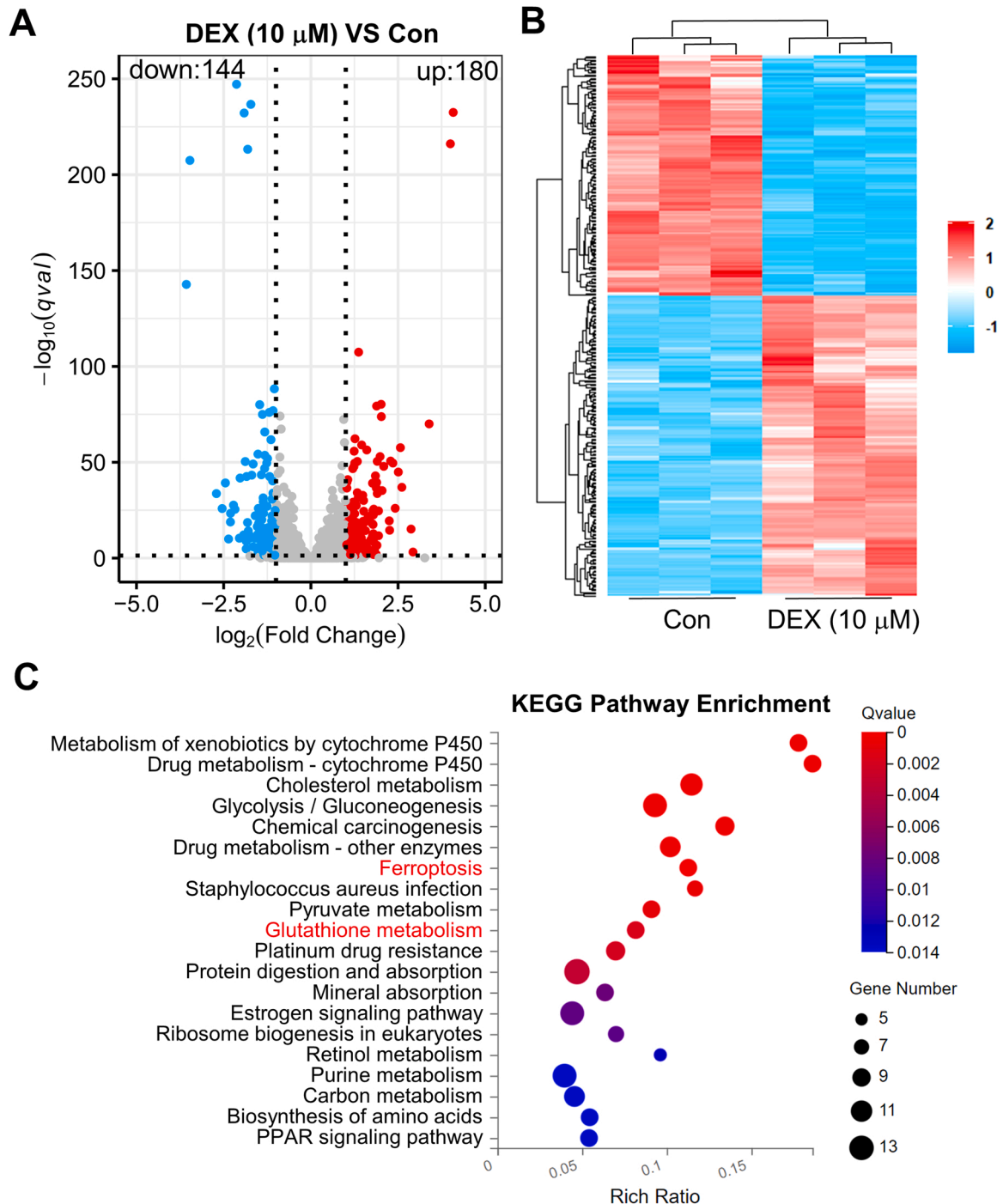


Fig. 2. Transcriptomic analysis of the gene expression in 5 dpf larvae treated with DEX for 48 h. (A) Volcano plot showing the differentially expressed genes in response to DEX treatment (Fold change ≥ 2 or ≤ 0.5 , Q value ≤ 0.05). (B) Heat map showing the differentially expressed genes. (C) KEGG pathway enrichment analysis of the differentially expressed genes.

system (Bio-Rad, California, USA). The PCR protocol was mentioned in a previous study (Xia et al., 2018). The PCR cycle was listed as follows: denaturation for 1 min at 95 °C, followed by 40 cycles of 15 s at 95 °C and 1 min at 60 °C. The primers were listed in Table S1 (Sarkar et al., 2014; Holowiecki et al., 2016; Ji et al., 2013; Hartig et al., 2016).

2.12. Fer-1, NAC and GSH treatments

Larvae at 3 dpf were exposed to 10 μ M of DEX together with desired concentrations of Fer-1, NAC or GSH, at a density of 30 larvae/well in 3 ml E3 medium for 48 h. Quantifications of T cells and vertebrae were

performed according to the protocols mentioned above.

2.13. Statistical analysis

All data in the present study were expressed as means \pm SE. For single DEX exposure, comparisons were performed between the DEX-treated groups and the control group. For the groups treated with DEX and DEX together with Fer-1, NAC or GSH simultaneously, comparisons were performed between the DEX-treated group and the other groups. The statistics were analyzed using ANOVA followed by Dunnett's multiple comparisons test by GraphPad Prism 7. *, $p < 0.05$; **, $p < 0.01$;

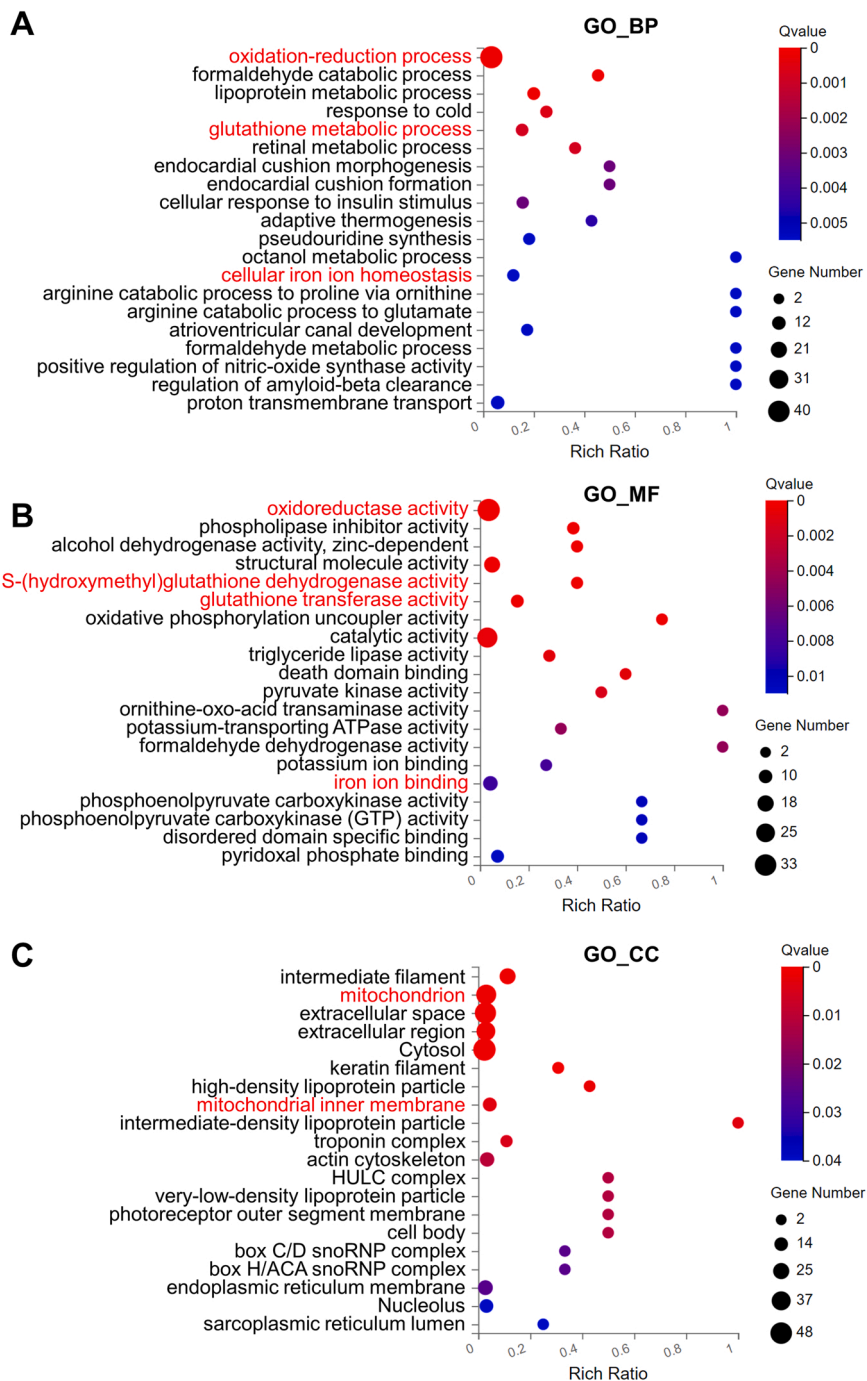


Fig. 3. GO analysis against the differentially expressed genes in 5 dpf larvae treated with DEX for 48 h. (A) Top 20 affected BP by DEX. (B) Top 20 affected MF by DEX. (C) Top 20 affected CC by DEX.

***, $p < 0.001$.

3. Results

3.1. DEX induced T cell ablation and osteoporosis in larval zebrafish

As shown in Fig. 1A, DEX induced T cell ablation at all tested concentrations. The quantitative results showed that DEX significantly suppressed T cell proliferation in a dose-dependent manner (Fig. 1B), indicating that DEX induced immune suppression in zebrafish larvae.

As shown in Fig. 1C, DEX inhibited the skeletal mineralization in zebrafish larvae. The numbers of mineralized vertebrae were

significantly decreased in the 10, 30 and 100 μM groups, compared with the control group (Fig. 1D). Alizarin red staining further confirmed the results that DEX inhibited skeletal mineralization (Fig. S1A, B). In addition, the craniofacial bone mass decreased significantly after exposure to 30 and 100 μM of DEX (Fig. S1C, D). However, DEX exposure did not affect the development of craniofacial cartilage in zebrafish larvae (Fig. S1E, F). These results suggested that DEX induced osteoporosis in zebrafish larvae.

Immune response and osteoblast development have been demonstrated to contribute to the regeneration of the caudal fin in zebrafish (Brandão et al., 2019; Gu et al., 2020). Based on the caudal fin amputation model, we observed that DEX significantly suppressed the

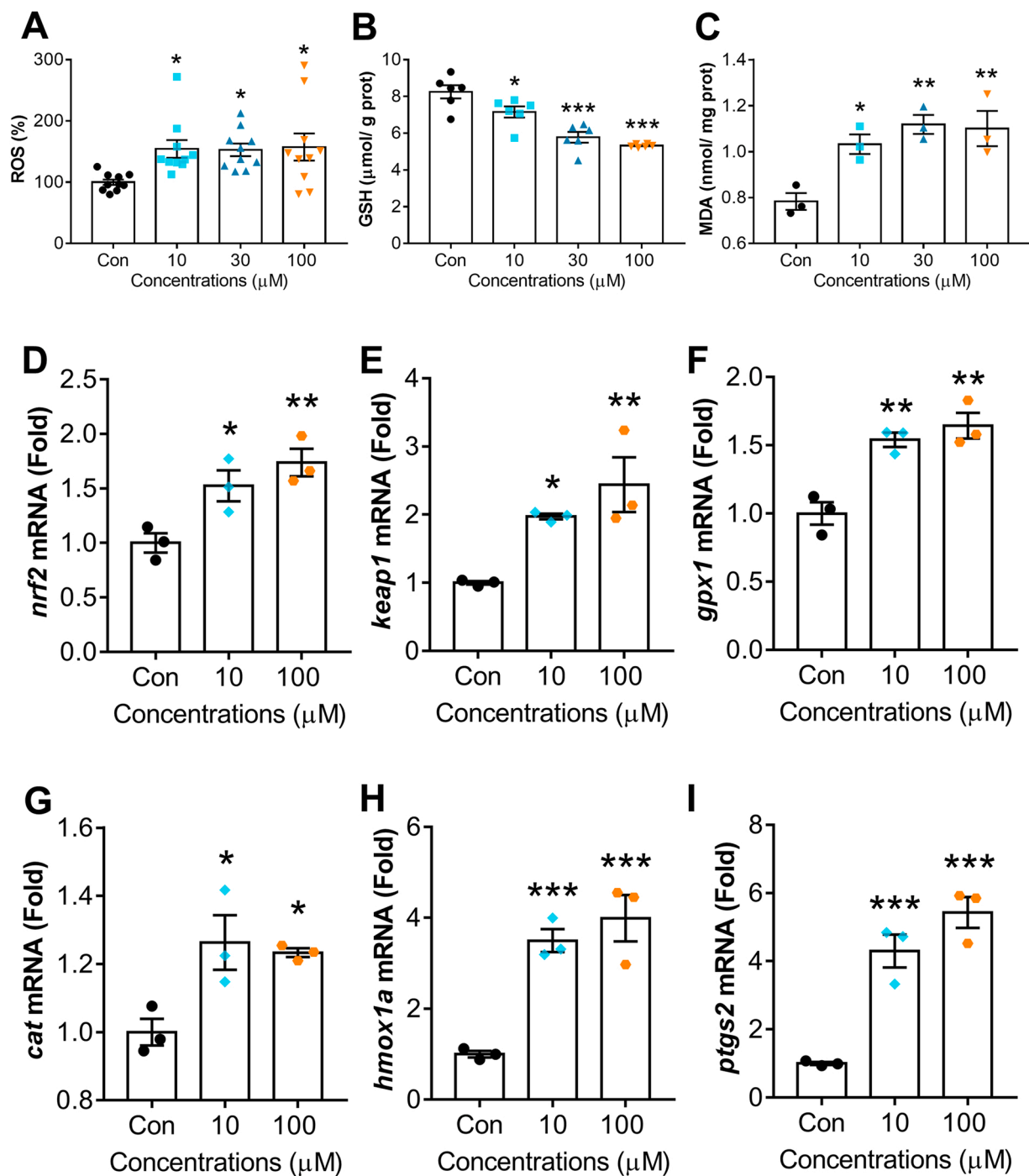


Fig. 4. Verification of the results indicated by the transcriptomic analysis. (A) The relative ROS levels in 5 dpf larvae treated with DEX for 48 h, $n = 10$. (B) GSH contents in 5 dpf larvae treated with DEX for 48 h, $n = 6$. (C) MDA contents in 5 dpf larvae treated with DEX for 48 h, $n = 3$. (D-I) The relative mRNA levels of *nrf2* (D), *keep1* (E), *gpx1* (F), *cat* (G), *hmox1a* (H) and *ptgs2* (I) in 5 dpf larvae treated with DEX for 48 h, $n = 3$. Data were shown as means \pm SE. * $p < 0.05$, ** $p < 0.01$, *** $p < 0.001$, compared with the control group.

regeneration of the caudal fin of zebrafish larvae (Fig. S2A, B), which further proved the disruptive effects of DEX on the immune and skeletal systems in zebrafish larvae. The possibility that the toxic effects of DEX on immune and skeletal systems were attributed to developmental toxicity was ruled out, as no malformation or shortened body length was observed in the DEX-treated larvae (Fig. S2C, D).

3.2. DEX induced ferroptosis and oxidative stress in zebrafish larvae

RNA-sequencing and transcriptomic analysis were performed to

investigate the mechanisms underlying the DEX-induced toxic effects in zebrafish larvae. The sequencing data were validated by the q-PCR results of several selected genes (Fig. S3). As shown in Fig. 2A, 180 genes were up-regulated and 144 genes were down-regulated (Fold Change ≥ 2 or ≤ 0.5 , $Q \text{ value} \leq 0.05$) in the larvae exposed to 10 μM of DEX for 48 h. Differentially expressed genes induced by DEX in each biological replicates from the same groups clustered together through hierarchical clustering (Fig. 2B). To explore the potential mechanisms involved in DEX-induced T cell ablation and osteoporosis, KEGG pathway enrichment was performed. Interestingly, the results implied that a newly

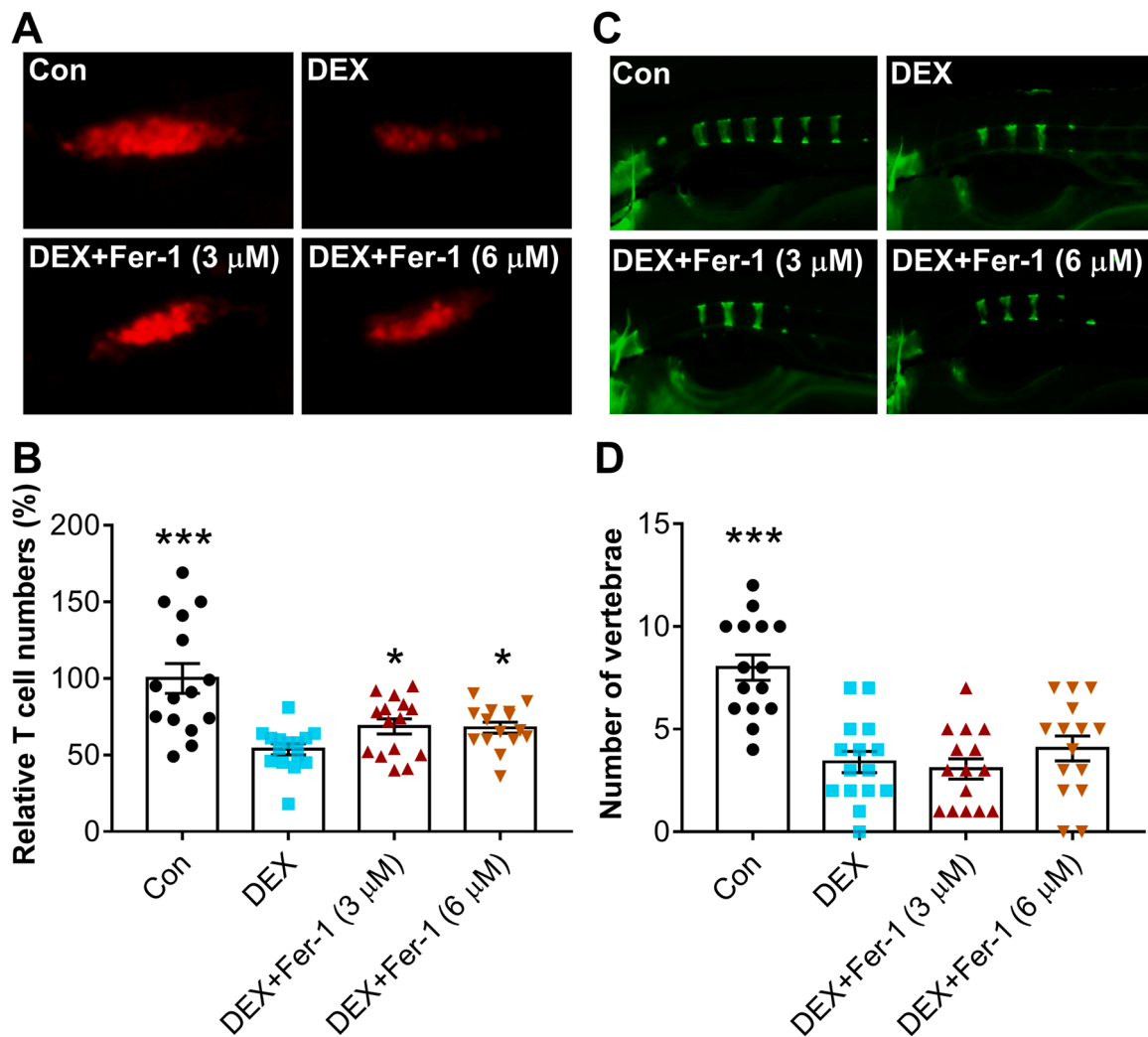


Fig. 5. Effects of Fer-1 on the DEX-induced T cell ablation and osteoporosis. (A) Representative images of the thymus of 5 dpf larvae treated with DEX and Fer-1 for 48 h. (B) Quantitative data of (A), $n = 15$. (C) Representative images of the vertebrae stained by calcein in 5 dpf larvae treated with DEX and Fer-1 for 48 h. (D) Quantitative data of (C), $n = 15$. Data were shown as means \pm SE. * $p < 0.05$, *** $p < 0.001$, compared with the DEX treated group.

identified death mode, ferroptosis might play a role in the DEX-induced toxic effects (Fig. 2C). In addition, the glutathione metabolism pathway was also significantly disrupted (Fig. 2C), which has been demonstrated to be an important inducement of ferroptosis (Sun et al., 2018).

Furthermore, GO analysis was executed to explore the biological process (BP), molecular function (MF) and cellular component (CC) associated with the DEX-induced toxic effects. The oxidation-reduction process was the leading affected BP. Glutathione metabolic process and cellular iron ion homeostasis were also altered by DEX exposure (Fig. 3A). In MF, oxidoreductase activity, S-(hydroxymethyl)-glutathione dehydrogenase activity, glutathione transferase activity and iron ion binding were dysregulated (Fig. 3B). Moreover, in CC, mitochondrion and mitochondrial inner membrane were associated with the DEX-induced toxic effects (Fig. 3C).

To verify the results obtained from the transcriptomic analysis, ROS, GSH, MDA and the genes related to ferroptosis and oxidative stress were measured. As shown in Fig. 4A, DEX significantly induced the production of ROS at 10, 30 and 100 μ M. The GSH contents were remarkably decreased in DEX-exposed groups, in a dose-dependent manner (Fig. 4B). Moreover, the well-demonstrated marker of ferroptosis (Lei et al., 2019; Tang et al., 2021), MDA contents were significantly increased in the DEX-treated groups (Fig. 4C). The key sensor of oxidative stress, Nrf2/Keap1 signal pathway was activated by DEX, evidenced by the up-regulation of mRNA levels of nrf2, keap1, gpx1 and

cat (Fig. 4D, E, F, G). Additionally, DEX treatment robustly elevated the mRNA levels of hmoxa and ptgs2 (Fig. 4H, I), the putative markers of ferroptosis (Yang et al., 2014; Fang et al., 2019). Because ferroptosis is an iron ion-dependent, oxidative stress-driven cell death, which showed specific characteristics of mitochondria (Jiang et al., 2021), all the results strongly suggested that DEX exposure induced ferroptosis in larval zebrafish.

3.3. Inhibition of ferroptosis partially attenuated the DEX-induced T cell ablation, but not osteoporosis in zebrafish larvae

To confirm the role of ferroptosis in DEX-induced T cells ablation and osteoporosis, the zebrafish larvae were treated with DEX and Fer-1 simultaneously. As shown in Fig. 5A and B, DEX treatment markedly reduced the T cells in the thymus of larvae, and the T cells were significantly increased in DEX/Fer-1 combined treatment groups. However, Fer-1 could not alleviate the DEX-induced osteoporosis in larval zebrafish (Fig. 5C, D). Interestingly, two well-known antioxidants, NAC and GSH alleviated both T cell ablation (Fig. 6A, B) and osteoporosis (Fig. 6C, D) induced by DEX.

4. Discussion

Natural and synthetic GCs exert their functions mostly through

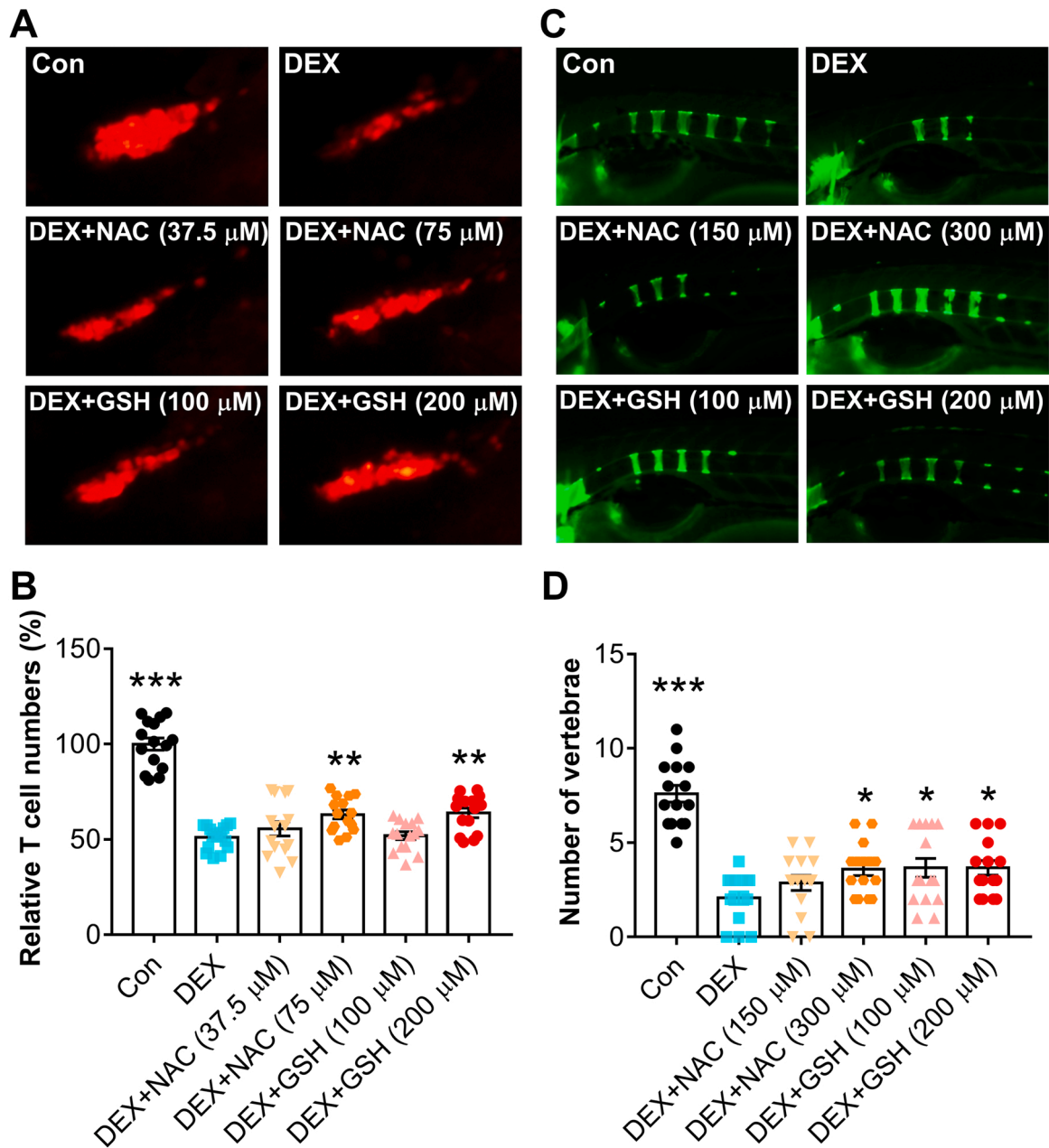


Fig. 6. Effects of NAC and GSH on the DEX-induced T cell ablation and osteoporosis. (A) Representative images of the thymus of 5 dpf larvae treated with DEX and NAC or GSH for 48 h. (B) Quantitative data of (A), $n = 15$. (C) Representative images of the vertebrae stained by calcein in 5 dpf larvae treated with DEX and NAC or GSH for 48 h. (D) Quantitative data of (C), $n = 15$. Data were shown as means \pm SE. * $p < 0.05$, ** $p < 0.01$, *** $p < 0.001$, compared with the DEX treated group.

activating the corresponding receptor, GR (Cain and Cidlowski, 2017). The GR is highly conserved in jawed vertebrates (Bridgham et al., 2006), and has been demonstrated to bind GCs in both mammals and fish (Hamilton et al., 2022). Although few data depicting the effects of GCs on fish are available, similar actions as observed in mammals are presumable, given the fact that the hypothalamic-pituitary-adrenal/hypothalamic-pituitary-interrenal (HPA/HPI) axis is well conserved in mammals and fish (Hamilton et al., 2022). As one of the predominant adverse effects found in mammals, GCs-induced immunosuppression in fish has been proved to be similar to that in mammals, such as the reduction of immune cells and the disruption of immune-related genes (Margiotta-Casaluci et al., 2016; Willi et al., 2019; Xie et al., 2021). It was observed that the T cells in the thymus reduced significantly after DEX treatment in the larval zebrafish (Fig. 1A, B). In agreement with our results, a previous study also demonstrated that the DEX effectively

ablated the T cells in 8 dpf zebrafish larvae (Langenau et al., 2004). Long-term use of GCs has been identified as the second cause of osteoporosis (Compston, 2018). We also found that DEX treatment reduced the number of calcein- or alizarin red-stained vertebrae, as well as the bone mass of craniofacial skeleton in zebrafish larvae (Fig. 1C, D; Fig. S1A, B, C, D), indicating that DEX-induced osteoporosis occurred. Consistent with our findings, other studies also reported that GCs induced osteoporosis in different bone tissues in zebrafish (Jiang et al., 2020; Chaichit et al., 2021).

Besides protecting the host from invading pathogens, the immune system has been demonstrated to play an essential role, either positive or negative, in the repair and regeneration processes (Mescher et al., 2017; Tsarouchas et al., 2018). Osteoblast development has also been demonstrated to contribute to the regeneration of the caudal fin in zebrafish (Gu et al., 2020). We hypothesized that if DEX exposure

influenced the immune and skeletal systems in zebrafish larvae, the regeneration process of the amputated caudal fin might be affected as well. As we expected, the regeneration of the amputated caudal fin of zebrafish larvae was significantly inhibited by DEX exposure (Fig. S2A, B), which further supported the result that DEX affected the immune and skeletal systems in zebrafish larvae. Although the immunotoxicity induced by the environmental chemicals has gained concern, the consequences of disruption of the immune system, such as defects in repair and regeneration, are still ignored in the risk assessment of environmental chemicals (Rehberger et al., 2017; Sun et al., 2019). Since physical trauma caused by aging, disease and other events is unavoidable, the capacity to repair their wound is critical for fish (Yoshinari and Kawakami, 2011). Our data together with others suggested that DEX could suppress the regeneration process in fish (Mathew et al., 2007), which might result in the unnatural death of fish, and consequently lead to the decline of the population.

Extensive efforts have been made to elucidate the mechanism underlying the GCs-induced adverse effects, yet the molecular mechanism is largely unknown (Schäcke et al., 2002; Ayroldi et al., 2014). In the present study, KEGG pathway enrichment analysis of the differentially expressed genes induced by DEX suggested that ferroptosis might be involved. In addition, GO analysis revealed that DEX exposure altered the biological processes and molecular functions related to iron ion homeostasis and glutathione metabolism (Fig. 3), which further strengthened the involvement of ferroptosis in DEX-induced toxic effects in zebrafish larvae. Ferroptosis is a newly identified form of iron-dependent programmed cell death, characterized by enhanced ROS, MDA and depleted GSH (Sun et al., 2018; Li et al., 2020), and has been proved to participate in numerous physiological and pathological processes (Jiang et al., 2021). In the current study, DEX exposure significantly elevated the ROS and MDA levels and reduced the GSH content in larval zebrafish (Fig. 4 A, B, C). In addition, the presumptive marker of ferroptosis, *ptgs2* was dramatically induced by DEX exposure in a dose-dependent manner (Fig. 4I). All these results strongly indicated that DEX exposure evoked ferroptosis in larval zebrafish.

Nrf2/Keap1 pathway is the vital protective system against oxidative stress (Kansanen et al., 2013). Recent studies have elucidated the tight relationship between ferroptosis and the Nrf2/Keap1 pathway (Lu et al., 2021). For instance, Nrf2 was demonstrated to mediate the DOX-induced ferroptosis in the heart of mice (Fang et al., 2019). Moreover, NRF2 is also reported to be a critical mitigator of both lipid peroxidation and ferroptosis. Activation of the Nrf2 pathway may infer the occurrence of ferroptosis (Dodson et al., 2019). Our data showed that Nrf2/Keap1 together with the downstream signals were activated by DEX exposure (Fig. 4), suggesting that the Nrf2/Keap1 pathway was involved in the DEX-induced ferroptosis in larval zebrafish.

Fer-1 is a small molecule inhibitor of ferroptosis (Dixon et al., 2012). In the present study, Fer-1 treatment partially attenuated the DEX-induced T cell ablation, but not osteoporosis (Fig. 5). Although the biochemical and molecular evidence indicated that DEX induced ferroptosis in zebrafish larvae, a marginal effect was observed on the T cells ablation after Fer-1 treatment. Because the biochemical and molecular parameters were detected by using the whole larvae, the ferroptosis might occur in other tissues besides the T cells and skeleton system. We speculated that ferroptosis may be involved in other toxic effects induced by DEX, as various GCs-induced side effects were reported previously (Huscher et al., 2009; Ayroldi et al., 2014). Briefly, our results demonstrated that DEX induced ferroptosis in larval zebrafish for the first time.

5. Conclusions

The present study confirmed the toxic effects of DEX exposure, including T cell ablation, osteoporosis and suppressed caudal fin regeneration in zebrafish larvae. In addition, DEX exposure induced ferroptosis in larval zebrafish. Furthermore, we proved that ferroptosis

partially participated in the DEX-induced T cell ablation, but not osteoporosis. These results provided compelling evidence that DEX might adversely affect the immune and skeleton system in fish, which further damage the regeneration process. In addition, our data gave an insight into the mechanism involved in DEX-induced toxicity in aquatic organisms, which might provide a new direction to study the toxicity induced by environmental chemicals.

CRedit authorship contribution statement

Wenyu Miao: Conceptualization, Methodology, Writing – original draft, Writing – review & editing, Funding acquisition. **Lingling He:** Methodology, Validation. **Yong Zhang:** Validation, Formal analysis. **Xiaoyu Zhu:** Methodology, Data curation. **Yangming Jiang:** Funding acquisition. **Pengpeng Liu:** Resources, Validation. **Tao Zhang:** Validation. **Chunqi Li:** Resources.

Declaration of Competing Interest

The authors declare that they have no known competing financial interests or personal relationships that could have appeared to influence the work reported in this paper.

Acknowledgments

The research was supported by Special Program for Technical Support of the State Administration for Market Regulation (2021YJ010) and The Open Fund of the Key Laboratory of Biosafety Detection for Zhejiang Market Regulation (2022BS001). We wish to thank Dr. Fudi Wang from Zhejiang University School of Medicine, for his valuable advice on experimental design.

Appendix A. Supporting information

Supplementary data associated with this article can be found in the online version at [doi:10.1016/j.ecoenv.2022.113872](https://doi.org/10.1016/j.ecoenv.2022.113872).

References

- Arnaldi, G., Scandali, V.M., Trementino, L., et al., 2010. Pathophysiology of dyslipidemia in Cushing's syndrome. *Neuroendocrinology* 92 (Suppl 1), 86–90.
- Askary, A., Mork, L., Paul, S., et al., 2015. Iroquois proteins promote skeletal joint formation by maintaining chondrocytes in an immature state. *Dev. Cell* 35 (3), 358–365.
- Ayroldi, E., Macchiarulo, A., Riccardi, C., 2014. Targeting glucocorticoid side effects: selective glucocorticoid receptor modulator or glucocorticoid-induced leucine zipper? A perspective. *FASEB J.* 28 (12), 5055–5070.
- Bamberg, E., Palme, R., Meingassner, J.G., 2001. Excretion of corticosteroid metabolites in urine and faeces of rats. *Lab Anim.* 35 (4), 307–314.
- Bambino, K., Chu, J., 2017. Zebrafish in toxicology and environmental health. *Curr. Top. Dev. Biol.* 124, 331–367.
- Brandão, A.S., Bensimon-Brito, A., Lourenço, R., et al., 2019. Yap induces osteoblast differentiation by modulating Bmp signalling during zebrafish caudal fin regeneration. *J. Cell Sci.* 132 (22), jcs231993.
- Bridgham, J.T., Carroll, S.M., Thornton, J.W., 2006. Evolution of hormone-receptor complexity by molecular exploitation. *Science* 312 (5770), 97–101.
- Cain, D.W., Cidlowski, J.A., 2017. Immune regulation by glucocorticoids. *Nat. Rev. Immunol.* 17 (4), 233–247.
- Chaichit, S., Sato, T., Yu, H., et al., 2021. Evaluation of dexamethasone-induced osteoporosis in vivo using zebrafish scales. *Pharm. (Basel)* 14 (6), 536.
- Chatzopoulou, A., Schoonheim, P.J., Torraca, V., Meijer, A.H., Spaink, H.P., Schaaf, M.J.M., 2017. Functional analysis reveals no transcriptional role for the glucocorticoid receptor β -isoform in zebrafish. *Mol. Cell. Endocrinol.* 447, 61–70.
- Compston, J., 2018. Glucocorticoid-induced osteoporosis: an update. *Endocrine* 61 (1), 7–16.
- Da Silva, J.A., Jacobs, J.W., Kirwan, J.R., et al., 2006. Safety of low dose glucocorticoid treatment in rheumatoid arthritis: published evidence and prospective trial data. *Ann. Rheum. Dis.* 65, 285–293.
- de Vrieze, E., van Kessel, M.A., Peters, H.M., Spanings, F.A., Flik, G., Metz, J.R., 2014. Prednisolone induces osteoporosis-like phenotype in regenerating zebrafish scales. *Osteoporos. Int* 25 (2), 567–578.
- Dixon, S.J., Lemberg, K.M., Lamprecht, M.R., Skouta, R., Zaitsev, E.M., Gleason, C.E., et al., 2012. Ferroptosis: an iron-dependent form of nonapoptotic cell death. *Cell* 149, 1060–1072.

- Dodson, M., Castro-Portuguez, R., Zhang, D.D., 2019. NRF2 plays a critical role in mitigating lipid peroxidation and ferroptosis. *Redox Biol.* 23, 101107.
- Du, S.J., Frenkel, V., Kindschi, G., Zohar, Y., 2001. Visualizing normal and defective bone development in zebrafish embryos using the fluorescent chromophore calcein. *Dev. Biol.* 238, 239–246.
- Fang, X., Wang, H., Han, D., et al., 2019. Ferroptosis as a target for protection against cardiomyopathy. *Proc. Natl. Acad. Sci. USA* 116 (7), 2672–2680.
- Formella, L., Svahn, A.J., Radford, R.A.W., Don, E.K., Cole, N.J., Hogan, A., Lee, A., Chung, R.S., Morsch, M., 2018. Real-time visualization of oxidative stress-mediated neurodegeneration of individual spinal motor neurons in vivo. *Redox Biol.* 19, 226–234.
- Grossi, O., Genereau, T., 2013. Glucocorticoids and infections, doping, surgery, sexuality. *Rev. Med Interne* 34, 269–278.
- Gu, L., Tian, L., Gao, G., et al., 2020. Inhibitory effects of polystyrene microplastics on caudal fin regeneration in zebrafish larvae. *Environ. Pollut.* 266 (Pt 3), 114664.
- Hamilton, C.M., Winter, M.J., Margiotta-Casaluci, L., Owen, S.F., Tyler, C.R., 2022. Are synthetic glucocorticoids in the aquatic environment a risk to fish? *Environ. Int.* 162, 107163.
- Hartig, E.I., Zhu, S., King, B.L., Coffman, J.A., 2016. Cortisol-treated zebrafish embryos develop into pro-inflammatory adults with aberrant immune gene regulation. *Biol. Open* 5 (8), 1134–1141.
- Hill, A.J., Teraoka, H., Heideman, W., Peterson, R.E., 2005. Zebrafish as a model vertebrate for investigating chemical toxicity. *Toxicol. Sci.* 86 (1), 6–19.
- Holowiecki, A., O'Shields, B., Jenny, M.J., 2016. Characterization of heme oxygenase and biliverdin reductase gene expression in zebrafish (*Danio rerio*): Basal expression and response to pro-oxidant exposures. *Toxicol. Appl. Pharm.* 311, 74–87.
- Huscher, D., Thiele, K., Gromnica-Ihle, E., et al., 2009. Dose-related patterns of glucocorticoid-induced side effects. *Ann. Rheum. Dis.* 68, 1119–1124.
- Ji, K., Liu, X., Lee, S., et al., 2013. Effects of non-steroidal anti-inflammatory drugs on hormones and genes of the hypothalamic-pituitary-gonad axis, and reproduction of zebrafish. *J. Hazard Mater.* 254–255, 242–251.
- Jia, A., Wu, S., Daniels, K.D., Snyder, S.A., 2016. Balancing the budget: accounting for glucocorticoid bioactivity and fate during water treatment. *Environ. Sci. Technol.* 50, 2870–2880.
- Jiang, X., Stockwell, B.R., Conrad, M., 2021. Ferroptosis: mechanisms, biology and role in disease. *Nat. Rev. Mol. Cell Biol.* 22, 266–282.
- Jiang, Y., Lu, Y., Jiang, X., et al., 2020. Glucocorticoids induce osteoporosis mediated by glucocorticoid receptor-dependent and -independent pathways. *Biomed. Pharm.* 125, 109979.
- Kansanen, E., Kuosmanen, S.M., Leinonen, H., Levonen, A.L., 2013. The Keap1-Nrf2 pathway: Mechanisms of activation and dysregulation in cancer. *Redox Biol.* 1 (1), 45–49.
- Katsu, Y., Oka, K., Baker, M.E., 2018. Evolution of human, chicken, alligator, frog, and zebrafish mineralocorticoid receptors: Allosteric influence on steroid specificity. *Sci. Signal* 11 (537), eaao1520.
- Langenau, D.M., Ferrando, A.A., Traver, D., et al., 2004. In vivo tracking of T cell development, ablation, and engraftment in transgenic zebrafish. *Proc. Natl. Acad. Sci. USA* 101 (19), 7369–7374.
- Lei, P., Bai, T., Sun, Y., 2019. Mechanisms of ferroptosis and relations with regulated cell death: A review. *Front. Physiol.* 10, 139.
- Li, J., Cao, F., Yin, H.L., et al., 2020. Ferroptosis: past, present and future. *Cell Death Dis.* 11 (2), 88.
- Lisco, G., Giagulli, V.A., Iovino, M., Guastamacchia, E., Pergola, G., Triggiani, V., 2021. Endocrine-disrupting chemicals: introduction to the theme. *Endocr. Metab. Immune Disord. Drug Targets* 2021.
- Liu, D., Ahmet, A., Ward, L., et al., 2013. A practical guide to the monitoring and management of the complications of systemic corticosteroid therapy. *Allergy Asthma Clin. Immunol.* 9 (1), 30.
- Lu, J., Zhao, Y., Liu, M., Lu, J., Guan, S., 2021. Toward improved human health: Nrf2 plays a critical role in regulating ferroptosis. *Food Funct.* 12 (20), 9583–9606.
- Macikova, P., Groh, K.J., Ammann, A.A., Schirmer, K., Suter, M.J.F., 2014. Endocrine disrupting compounds affecting corticosteroid signaling pathways in Czech and Swiss waters: potential impact on fish. *Environ. Sci. Technol.* 48, 12902–12911.
- Margiotta-Casaluci, L., Owen, S.F., Huerta, B., Rodríguez-Mozaz, S., Kugathas, S., Barceló, D., Rand-Weaver, M., Sumpster, J.P., 2016. Internal exposure dynamics drive the Adverse Outcome Pathways of synthetic glucocorticoids in fish. *Sci. Rep.* 6, 21978.
- Mescher, A.L., Neff, A.W., King, M.W., 2017. Inflammation and immunity in organ regeneration. *Dev. Comp. Immunol.* 66, 98–110.
- Mommsen, T.P., Vijayan, M.M., Moon, T.W., 1999. Cortisol in teleosts: Dynamics, mechanisms of action, and metabolic regulation. *Rev. Fish. Biol. Fish.* 9, 211–268.
- Olefsky, J.M., Kimmeling, G., 1976. Effects of glucocorticoids on carbohydrate metabolism. *Am. J. Med. Sci.* 271 (2), 202–210.
- Piper, J.M., Ray, W.A., Daugherty, J.R., Griffin, M.R., 1991. Corticosteroid use and peptic ulcer disease: role of nonsteroidal anti-inflammatory drugs. *Ann. Intern Med.* 114, 735–740.
- Qi, X.Z., Tu, X., Zha, J.W., Huang, A.G., Wang, G.X., Ling, F., 2019. Immunosuppression-induced alterations in fish gut microbiota may increase the susceptibility to pathogens. *Fish. Shellfish Immunol.* 88, 540–545.
- Rehberger, K., Werner, L., Hitzfeld, B., Segner, H., Baumann, L., 2017. 20 years of fish immunotoxicology - what we know and where we are. *Crit. Rev. Toxicol.* 47, 509–535.
- Rosa, J.T., Laizé, V., Gavaia, P.J., Cancela, M.L., 2021. Fish models of induced osteoporosis. *Front. Cell Dev. Biol.* 9, 672424.
- Sadr-Azodi, O., Mattsson, F., Bexlius, T.S., et al., 2013. Association of oral glucocorticoid use with an increased risk of acute pancreatitis: a population-based nested case-control study. *JAMA Intern Med.* 173, 444–449.
- Sarkar, S., Mukherjee, S., Chattopadhyay, A., Bhattacharya, S., 2014. Low dose of arsenic trioxide triggers oxidative stress in zebrafish brain: expression of antioxidant genes. *Ecotoxicol. Environ. Saf.* 107, 1–8.
- Schäcke, H., Döcke, W.D., Asadullah, K., 2002. Mechanisms involved in the side effects of glucocorticoids. *Pharm. Ther.* 96 (1), 23–43.
- Schakman, O., Gilson, H., Thissen, J.P., 2008. Mechanisms of glucocorticoid-induced myopathy. *J. Endocrinol.* 197 (1), 1–10.
- Spoorendonk, K.M., Peterson-Maduro, J., Renn, J., et al., 2008. Retinoic acid and Cyp26b1 are critical regulators of osteogenesis in the axial skeleton. *Development* 135 (22), 3765–3774.
- Stuck, A.E., Minder, C.E., Frey, F.J., 1989. Risk of infectious complications in patients taking glucocorticosteroids. *Rev. Infect. Dis.* 11, 954–963.
- Sun, L., Gu, L., Tan, H., et al., 2019. Effects of 17 α -ethinylestradiol on caudal fin regeneration in zebrafish larvae. *Sci. Total Environ.* 653, 10–22.
- Sun, Y., Zheng, Y., Wang, C., Liu, Y., 2018. Glutathione depletion induces ferroptosis, autophagy, and premature cell senescence in retinal pigment epithelial cells. *Cell Death Dis.* 9 (7), 753.
- Takahashi, H., Sakamoto, T., 2013. The role of “mineralocorticoids” in teleost fish: relative importance of glucocorticoid signaling in the osmoregulation and “central” actions of mineralocorticoid receptor. *Gen. Comp. Endocrinol.* 181, 223–228.
- Tang, D., Chen, X., Kang, R., Kroemer, G., 2021. Ferroptosis: molecular mechanisms and health implications. *Cell Res* 31 (2), 107–125.
- Tsarouchas, T.M., Wehner, D., Cavone, L., et al., 2018. Dynamic control of proinflammatory cytokines IL-1 β and Tnf- α by macrophages in zebrafish spinal cord regeneration. *Nat. Commun.* 9 (1), 4670.
- Van Staa, T.P., Leufkens, H.G., Abenhaim, L., Zhang, B., Cooper, C., 2000. Use of oral corticosteroids and risk of fractures. *J. Bone Min. Res* 15 (6), 993–1000.
- Wei, L., MacDonald, T.M., Walker, B.R., 2004. Taking glucocorticoids by prescription is associated with subsequent cardiovascular disease. *Ann. Intern Med.* 141, 764–770.
- Weinstein, R.S., 2012. Glucocorticoid-induced osteoporosis and osteonecrosis. *Endocrinol. Metab. Clin. North Am.* 41 (3), 595–611.
- Willi, R.A., Faltermann, S., Hettich, T., Fent, K., 2018. Active glucocorticoids have a range of important adverse developmental and physiological effects on developing zebrafish embryos. *Environ. Sci. Technol.* 52, 877–885.
- Willi, R.A., Salgueiro-González, N., Carcasio, G., Fent, K., 2019. Glucocorticoid mixtures of fluticasone propionate, triamcinolone acetonide and clobetasol propionate induce additive effects in zebrafish embryos. *J. Hazard. Mater.* 374, 101–109.
- Xia, J., Lu, L., Jin, C., Wang, S., Zhou, J., Ni, Y., Fu, Z., Jin, Y., 2018. Effects of short term lead exposure on gut microbiota and hepatic metabolism in adult zebrafish. *Comp. Biochem. Physiol. C. Toxicol. Pharm.* 209, 1–8.
- Xie, Y., Xie, J., Meijer, A.H., Schaaf, M.J.M., 2021. Glucocorticoid-Induced Exacerbation of Mycobacterial Infection Is Associated With a Reduced Phagocytic Capacity of Macrophages. *Front. Immunol.* 12, 1–15.
- Yang, W.S., et al., 2014. Regulation of ferroptotic cancer cell death by GPX4. *Cell* 156, 317–331.
- Yoshinari, N., Kawakami, A., 2011. Mature and juvenile tissue models of regeneration in small fish species. *Biol. Bull.* 221, 62–78.
- Zhang, J., Yang, Y., Liu, W., Schlenk, D., Liu, J., 2019. Glucocorticoid and mineralocorticoid receptors and corticosteroid homeostasis are potential targets for endocrine-disrupting chemicals. *Environ. Int.* 133 (Pt A), 105133.
- Zhang, K., Zhao, Y., Fent, K., 2017. Occurrence and ecotoxicological effects of free, conjugated, and halogenated steroids including 17 α -hydroxypregnanolone and pregnanediol in Swiss wastewater and surface water. *Environ. Sci. Technol.* 51 (11), 6498–6506.
- Zhang, P., He, Q., Chen, D., et al., 2015. G protein-coupled receptor 183 facilitates endothelial-to-hematopoietic transition via Notch1 inhibition. *Cell Res* 25 (10), 1093–1107.
- Zhao, Y., Zhang, K., Fent, K., 2016. Corticosteroid fludrocortisone acetate targets multiple end points in zebrafish (*Danio rerio*) at low concentrations. *Environ. Sci. Technol.* 50, 10245–10254.